The $E, F\ ^1\Sigma_g^+$ double-minimum state of hydrogen: Two-photon excitation of inner and outer wells[a)]

E. E. Marinero, R. Vasudev, and R. N. Zare[b)]

Department of Chemistry, Stanford University, Stanford, California 94305
(Received 10 August 1982; accepted 11 October 1982)

Low-lying vibrational levels ($v = 2$ and 3) of the outer well of the double-minimum $E, F\ ^1\Sigma_g^+$ state of molecular hydrogen are experimentally observed for the first time permitting a rotational analysis. The E, F state is excited by two-photon absorption using tunable (~195 nm) Raman-shifted radiation of a frequency-doubled dye laser. The nonlinear absorption is detected by monitoring the subsequent photoionization of the E, F state. Homogeneous perturbations are observed between the $v_E = 1$ and $v_F = 2$ levels of the inner and outer wells, respectively. The molecular parameters for these levels (derived by a deperturbation analysis) as well as those for the unperturbed $v_F = 3$ level are compared with recent *ab initio* calculations and small deviations are noted. The rotational intensity distribution of the E–X (0,0) band mirrors the ground state rotational population, whereas the corresponding distributions of the E–X (1,0) and (2,0) bands as well as the F-X (4,0) band do not follow this pattern. This is interpreted in terms of vibronic coupling between the inner and outer wells of the E, F state. A comparison between the experimental rotationless intensities and those calculated from *ab initio* ground and excited state vibrational wave functions suggests that photoionization from the outer well is more effective than from the inner well.

I. INTRODUCTION

The first excited $^1\Sigma_g^+$ state of H_2 represents one of the few well established examples of a diatomic potential curve having two wells, both of which support bound vibrational levels.[1] As such, this state is the subject of much interest and curiosity, especially so because the hydrogen molecule is sufficiently simple to permit rather complete *ab initio* calculations to be carried out on its structure. The origin of this double-minimum behavior may be traced to an avoided curve crossing.[2] In the valence bond framework the two interacting electronic states of the same symmetry are the $H^+ + H^-$ and $H(1s) + H(2s)\ ^1\Sigma_g^+$ states. In the molecular orbital picture the inner well, called the E state, is predominantly described by the $(1s\sigma_g)(2s\sigma_g)$ configuration, while the outer well, called the F state, is mostly described by the doubly excited $(2p\sigma_u)^2$ configuration with some contributions from the $(1s\sigma_g)(2s\sigma_g)$ configuration and the ground state $(1s\sigma_g)^2$ configuration. The H_2, E, F state is also of special interest because it is the upper state of a number of prominent emission bands in the H_2 visible spectrum, first studied by Richardson[3] and by Dieke and co-workers.[4–8] Dieke assigned the observed transitions to two separate band systems, now known as $E\ ^1\Sigma_g^+$–$B\ ^1\Sigma_u^+$ and $F\ ^1\Sigma_g^+$–$B\ ^1\Sigma_u^+$. However, the theoretical work of Davidson[2] clearly established the E, F state as having a double-minimum structure and this conclusion has been fully confirmed by the more extensive theoretical studies of Kołos, Wolniewicz, Dressler, and others.[9–11]

The inner well has its minimum near 1.012 Å while that of the outer well occurs near 2.322 Å. The two wells are separated by a potential barrier of about 6700 cm^{-1} which reaches its maximum around 1.651 Å. Because the equilibrium bond lengths of the E and F states are so different, the potential energy curves near r_e largely retain their original (Born–Oppenheimer) character and their homogeneous ($\Delta\Lambda = 0$) interactions are weak. Far from r_e, however, the states are extensively mixed. According to the best quantum calculations[9–11] the inner $E\ ^1\Sigma_g^+$ well contains three vibrational levels ($v_E = 0$–2), whereas five vibrational levels ($v_F = 0$–4) are confined in the outer $F\ ^1\Sigma_g^+$ well. Above the potential barrier, on the other hand, it is not possible to associate the vibrational levels as belonging uniquely to either the E or the F wells. Dieke's extensive experimental work, which actually preceded the aforementioned *ab initio* papers, has firmly established all the vibrational levels of the inner well, the $v_F = 4$ level of the outer well, and some higher levels of the E, F mixture above the potential barrier. Evidence for the existence of the $v_F = 2$ level has been inferred only indirectly from inhomogeneous perturbations in the $v_E = 1$ level,[5] whereas for the $v_F = 0$, 1, and 3 levels no experimental corroboration exists, either in discharge[3–8] or in electron impact excitation[12] studies.

For the fully isotopically substituted molecules D_2 and T_2 Dieke and Cunningham[7] also observed transitions from the inner and outer wells of the E, F state to the B state. However, for the isotopically asymmetrized molecule HD weak $^1\Sigma_g^+$–$^1\Sigma_g^+$ transitions occur because the $g \not\leftrightarrow g$ prohibition only holds in the Born–Oppenheimer approximation. This has permitted Dabrowski and Herzberg[13] to observe and analyze a number of bands from the ground state to both the inner and outer wells of the E, F state for this molecule.

An alternative approach, based on two-photon excitation, is used in this work to observe directly the $v_F = 2$ and 3 levels of the outer well of H_2. According to the *ab*

[a)]Supported financially by the Office of Naval Research under N00014-C-78-0403 and the National Science Foundation under NSF CHE 81-08823.

[b)]R. N. Z. gratefully akknowledges support through the Shell Distinguished Chairs program, funded by the Shell Companies Foundation, Inc.

 0021-9606/83/020692-08$2.10

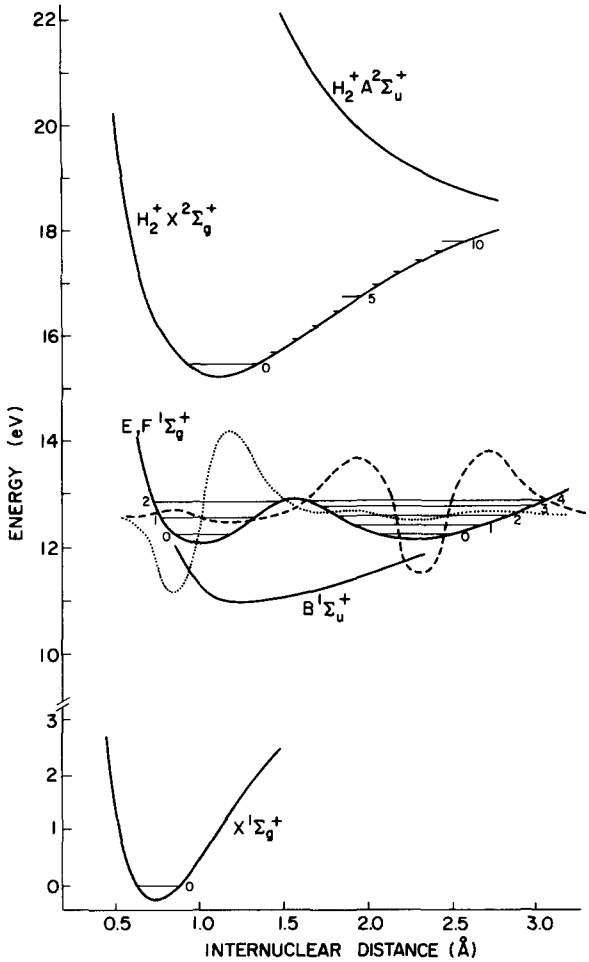

FIG. 1. Potential energy curves for some of the electronic states of H_2 and H_2^+. Also shown are the *ab initio* vibrational wave functions, taken from Kołos and Wolniewicz (Ref. 9) for $v=1$ of the $E\ ^1\Sigma_g^+$ state (dotted line) and $v=2$ of the $F\ ^1\Sigma_g^+$ state (dashed line). To avoid congestion, the $C\ ^1\Pi_u$ potential energy curve (which is nearly coincident with $E\ ^1\Sigma_g^+$) is not shown.

initio calculations of Kołos and Wolniewicz,[9] the vibrational wave functions of the outer well show a small but significant tunneling into the inner well and thus into the region corresponding to the ground state ($X^1\Sigma_g^+$) equilibrium bond length (see Fig. 1). Consequently, there is a weak vibrational overlap with the vibrationless level ($v_X=0$) of the ground state. The $^1\Sigma_g^+ - ^1\Sigma_g^+$ transition is, of course, forbidden in one-photon electric dipole absorption, but is allowed in a two-photon (TP) process.

The TP excitation of the $E,\ F\ ^1\Sigma_g^+$ state can be detected via subsequent emission to the $B^1\Sigma_u^+$ state, as first demonstrated by Kligler *et al.*[14] for the (2,0) band of the $E-X$ system. Using a tunable ArF excimer laser, these investigators measured the excited state radiative lifetime (100 ± 20 ns) and estimated the photoionization cross section ($\sim 10^{-18}$ cm^2). Under tight-focusing conditions ($I > 10^9$ W/cm^2), it follows from their studies that the photoionization of the $E,\ F$ state dominates radiative decay. This has been confirmed in the study of Marinero *et al.*[15] Since ions can be collected with nearly unit efficiency, we have chosen to use photoionization to detect TP transitions to various levels of the $E,\ F$ state. In particular, we have observed TP transitions to $v_E=0$, 1, and 2 and to $v_F=2$, 3, and 4. No evidence for $v_F=0$ or 1 is found within the present detection limits, which is consistent with their extremely small vibrational overlaps with the vibrationless ground state. A rotational analysis has been carried out on the $E-X$ (1,0) band and the $F-X$ (2,0) and (3,0) bands. The resulting band origins and upper state rotational constants are compared to the best available *ab initio* calculations. Small discrepancies with theory are found.

The TP intensity distributions for the (0,0), (1,0), and (2,0) bands of the $E-X$ system and the (2,0) and (4,0) bands of the $F-X$ system have also been measured at low H_2 pressures. While the rotational intensity distribution of the (0,0) band of the $E-X$ system mirrors the ground state rotational population,[15] the corresponding distributions of the (1,0) and (2,0) bands of the $E-X$ system as well as the (2,0) and (4,0) bands of the $F-X$ system do not follow this pattern. These deviations are interpreted in terms of vibronic coupling between the levels of the inner and outer wells of the $E,\ F$ state. From the relative intensities of members of the Q and S branches, an estimate is made of the contributions of $B^1\Sigma_u^+$ and $C^1\Pi_u$ to the virtual intermediate states in the two-photon process under study.

II. EXPERIMENTAL

The experimental setup used in the present work is very similar to that reported previously.[15] Briefly, the output of a pulsed dye laser, pumped by the second harmonic of a Nd:YAG laser, is frequency doubled using KD*P crystals (Quanta-Ray DCR/PDL/WEX system). The doubled output together with the fundamental are then Raman-shifted in a high-pressure (95–120 psi) H_2 cell. The fourth anti-Stokes of the doubled dye laser output, which constitutes the excitation source, is first separated from all other unwanted frequencies by a Pellin–Broca prism and, after spatial filtering, is focused into the ionization chamber. Two-photon transition energies between 98 800 and 104 000 cm^{-1} are scanned by tuning the dye laser in the range 565–610 nm. Typical fourth anti-Stokes output energies are between 10 and 20 μJ per pulse. The excitation bandwidth is measured to be ~ 0.9 cm^{-1}.

The ions are collected using a conventional parallel-plate arrangement, with the repeller biased between 50–1000 V. The ion current is either directly, or after preamplification, processed by a boxcar averager (PAR 162/164). To calibrate the fourth anti-Stokes pumping wavelength, we record the fluorescence excitation of the NO $A^2\Sigma^+ - X^2\Pi$ system[16] with the *third* anti-Stokes of the doubled dye laser output (Raman shifting in H_2 generates adjacent orders separated by 4155.201 cm^{-1}).[17] A typical scan is shown in Fig. 2. The measurement accuracy of the H_2 line *centers* is estimated to be ~ 0.25 cm^{-1}.

III. RESULTS AND DISCUSSION

A. Rotational analysis

Two-photon spectra of the H_2 $E,\ F-X$ system in the region 99 160–104 000 cm^{-1} above the vibrationless

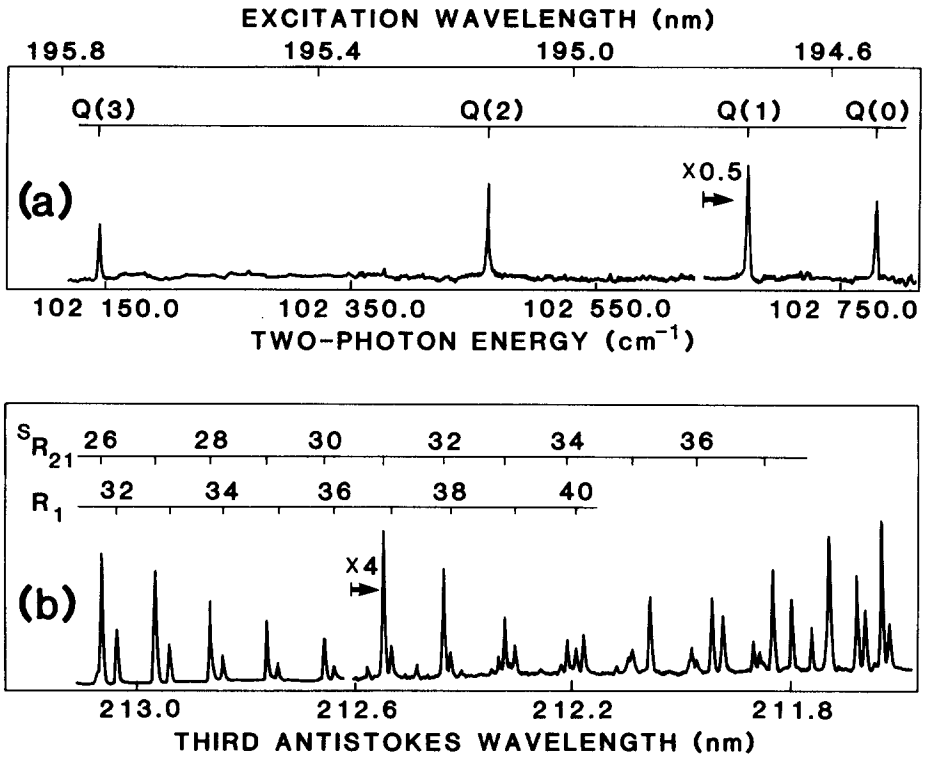

FIG. 2. Typical spectrum showing (a) the F–X (3,0) two-photon resonances in the multiphoton ionization of H_2 (unnormalized spectrum, sample pressure 95 Torr) and (b) fluorescence excitation spectrum of the (1,0) band of the NO $A\ ^2\Sigma^+$–$X\ ^2\Pi$ system recorded simultaneously with the third anti-Stokes radiation and used for calibration purposes.

ground state have been measured. Portions of these spectra together with their assignments are shown in Figs. 2 and 3. These spectra are recorded using a sample pressure of 95 Torr and consist predominantly of Q lines. Members of the S branch, being ~30 times weaker at this pressure, are observed only for the E–X (1,0) transition. Those of the O branches are still weaker due to unfavorable Boltzmann factors. The assign-

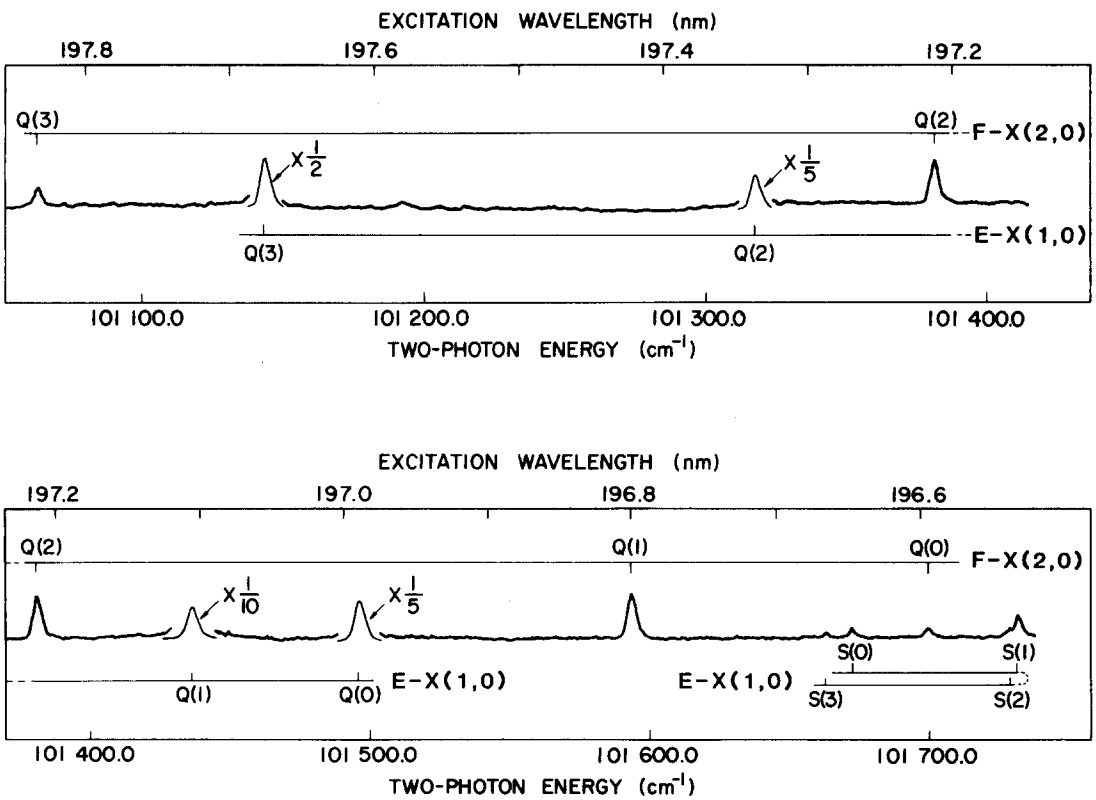

FIG. 3. The E–X (1,0) and F–X (2,0) resonances in the multiphoton ionization of H_2 (unnormalized spectrum, sample pressure 95 Torr).

TABLE I. Vacuum wave numbers (cm^{-1}) of the observed $E, F-X$ transitions.

	$E\ ^1\Sigma_g^+-X\ ^1\Sigma_g^+$		$F\ ^1\Sigma_g^+-X\ ^1\Sigma_g^+$	
	1–0		2–0	3–0
J	$Q(J)$	$S(J)$	$Q(J)$	$Q(J)$
0	101 494.80	101 671.41	101 699.02	102 777.71
1	101 435.35	101 730.85	101 592.30	102 671.37
2	101 317.17	101 726.68	101 380.51	102 459.23
3	101 143.71	101 661.66	101 062.93	102 143.72

ment of the observed lines as Q and S transitions is established on the basis of their relative intensities in linearly and circularly polarized excitations,[18,19] and is confirmed by the rotational analysis described below.

The measured line positions in all $E-X$ bands and the $F-X$ (4, 0) band agree satisfactorily with those obtained from Dieke's E, $F-B$ measurements[6] and the B-state term values.[20,21] Table I lists the line positions of the $F-X$(2, 0) and (3, 0) bands. For the $E-X$ system, only the (1, 0) lines are given as this band alone is used in our analysis.

In the first stage of the rotational analysis, the excited state term values $F_v(J)$ were generated using those of the vibrationless ground state, reported by Stoicheff.[17] The $F_v(J)$'s for each band were then fitted to the customary formula

$$F_v(J) = T_v + B_vJ(J+1) - D_vJ^2(J+1)^2 , \quad (1)$$

where, to eliminate the usual correlation between B_v and D_v due to lack of adequate data for light molecules, the D_v's were fixed at the value determined by the normally successful Kratzer formula $D_e = 4B_e^3/\omega_e^2$. For

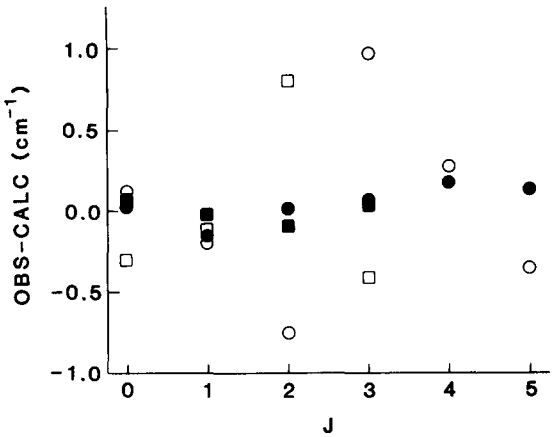

FIG. 4. Difference between the observed and the calculated term values vs J. ○ and □ refer to the fit of the $E\ ^1\Sigma_g^+$ $v=1$ and $F\ ^1\Sigma_g^+$ $v=2$ term values to Eq. (1); ● and ■ refer to the fit with the homogeneous perturbation term $W^{E,F}$ (1, 2) included (see the text).

$v_E=1$ and $v_F=2$, the fits were unsatisfactory since the calculated $J=2$ and 3 term values deviated from the observed ones by more than the measurement uncertainties, as shown in Fig. 4. Furthermore, the deviations for these two vibrational levels were in opposite directions, thus indicating a perturbation between them. A similar, though more severe, interaction was noted by Dieke[4,5] between the $v_E=2$ and $v_F=4$ levels. Perturbations between $v_E=1$ and $v_F=2$ are not entirely unexpected in view of their non-negligible vibrational overlap and their proximity (see Fig. 1).

In the deperturbation analysis presented here, we assume that the off-diagonal coupling matrix element

TABLE II. Comparison of observed and *ab initio* molecular parameters (cm^{-1}) for the H_2 $E, F\ ^1\Sigma_g^+$ state. The number in parentheses, attached to each constant, represents one standard deviation in the last figures quoted.

	$E\ ^1\Sigma_g^+$	$F\ ^1\Sigma_g^+$	
	$v=1$	$v=2$	$v=3$
	T_v		
Observed[a]	101 495.09(9)	101 698.64(11)	102 777.82(10)
Nonadiabatic calculation[b]	101 501	101 704	102 783
Adiabatic calculation[c]	101 501	101 706	102 787
	B_v		
Observed[a]	29.69(5)	5.90(2)	5.96(1)
Nonadiabatic calculation[b]	29.72	5.96	5.99
Adiabatic calculation[c]	29.73	5.96	5.99
Born–Oppenheimer calculation[c]	29.62	6.02	6.10

[a]This work.
[b]Dressler, Gallusser, Quadrelli, and Wolniewicz (Ref. 11).
[c]Wolniewicz and Dressler (Ref. 10).

$$W^{E,F}(1,2)=\langle v_E=1|\mathcal{H}'|v_F=2\rangle \quad (2)$$

is independent of J. For each J, the interacting $v_E=1$ and $v_F=2$ levels are then represented by a 2×2 matrix, defined by Eqs. (1) and (2). The results of a nonlinear least squares fit to the experimental term values are satisfactory, as shown in Fig. 4. The derived molecular parameters are listed in Table II, along with the *ab initio* values of Dressler *et al.*[10,11] The value of $W^{E,F}(1,2)$ is calculated to be 8.02 cm^{-1}, with a standard deviation of 0.32 cm^{-1}. The least squares fit has a standard deviation of 0.13 cm^{-1} for both the $v_E=1$, $v_F=2$ interacting pair and the unperturbed $v_F=3$ level. For the outer well, B_v *increases* with v, in contrast to normal behavior. This trend is caused by the fact that the F well opens more rapidly to smaller internuclear distances as the potential barrier is approached.

The comparison of the experimentally obtained B_v values with those from theory is highly instructive. It is seen at once that the Born–Oppenheimer approximation does not suffice, but that the adiabatic and nonadiabatic treatments give close agreement. However, we note that our experimental B_v values appear to be consistently smaller than the best theoretical values. Moreover, these deviations, which are three standard deviations for $v_F=2$ and 3, appear to be real. It is possible that a more extensive nonadiabatic calculation would remove this small discrepancy. Indeed, Dressler *et al.*[11] did not include the heterogeneous interactions of the E, $F\ ^1\Sigma_g^+$ state with the *higher* lying $^1\Pi_g$ states. Such interactions might be expected to decrease the theoretical B_v values. It is also possible that this difference can be narrowed by an improved interpolation of the potential energy and adiabatic corrections between the widely spaced internuclear distances for which the *ab initio* calculations were carried out.[22]

Table II also shows that the experimentally obtained band origins lie 5–6 cm^{-1} below the corresponding *ab initio* values. This discrepancy has been noted before and has been ascribed to a residual error in the calculated nonrelativistic Born–Oppenheimer energies.[11]

In spite of these discrepancies the overall agreement between theory and experiment is rather remarkable, indicating that we have a firm understanding of this unusual double-minimum excited state.

B. Rotational and vibronic intensity distributions

In this section, we consider the rotational intensity distributions within each E, F–X band. Such intensities are sensitive to *intra*molecular interactions and should therefore corroborate the perturbations described in the previous section. Furthermore, they are relevant to experiments in which ground state population distributions in H_2 are derived from two-photon signal amplitudes.[15]

Rotational line intensities of the E–X (0, 0), (1, 0), (2, 0) bands and the F–X (2, 0) and (4, 0) transitions, recorded at 295 K and 150 mTorr sample pressure, are given in Table III. Amplitudes are measured directly from the ion spectra and are corrected for variations in the excitation power. At these pressures and with power densities in excess of 10^9 W/cm^2, ionization should predominate over electronic quenching by ground state H_2 molecules, radiative decay and rotational relaxation.[14] This is verified in this work. In separate experiments we established the quadratic dependence of the ion signal on the excitation power.

The rotational intensity distribution within a given two-photon vibronic band depends, apart from the ground state populations, on the nature of the intermediate states. In order to describe quantitatively this dependence, it is necessary to summarize the essential portions of the theory of TP absorption,[18,19] particularly as it applies to the H_2 E, $F\ ^1\Sigma_g^+$–$X\ ^1\Sigma_g^+$ system. The intensity of a TP transition from the ground state $|G\rangle$ to the final two-photon state $\langle T|$ is governed by a transition tensor, whose Cartesian components are given by

$$S_{k,l}=\sum_I \frac{\langle T|\mu_k|I\rangle\langle I|\mu_l|G\rangle}{(E_I-E_G)-E_\omega+i\Gamma_I/2}\ , \quad (3)$$

where $|I\rangle$ is the "virtual" intermediate state and has contributions from all the vibronic states of the molecule; $(E_I-E_G)-E_\omega$ is the energy mismatch between the $|I\rangle \leftarrow |G\rangle$ transition and the excitation source frequency ω; μ_k and μ_l are the body-fixed Cartesian components of the electric dipole moment operator; and Γ_I is the homogeneous width of the intermediate state $|I\rangle$.

The rotational selection rules and line strengths are determined by the two dipole matrix elements of Eq. (3).[18,19] The relevant rotational line strength factors

TABLE III. Rotational line intensities[a] in the $E,F\ ^1\Sigma_g^+$–$X\ ^1\Sigma_g^+$ TP transition of H_2. The numbers in square brackets are the relative vibronic intensities calculated from the *ab initio* vibrational wave functions (see the text).

Rotational line	$E\ ^1\Sigma_g^+$–$X\ ^1\Sigma_g^+$ (0, 0)	$E\ ^1\Sigma_g^+$–$X\ ^1\Sigma_g^+$ (1, 0)	$E\ ^1\Sigma_g^+$–$X\ ^1\Sigma_g^+$ (2, 0)	$F\ ^1\Sigma_g^+$–$X\ ^1\Sigma_g^+$ (2, 0)	$F\ ^1\Sigma_g^+$–$X\ ^1\Sigma_g^+$ (4, 0)
$Q(0)$	6.2(3) [6]	21.8(5) [8]	9.4(3) [5]	0.25(2) [0.035]	2.7(2) [1.6]
$Q(1)$	27.3(8)	100.0(1.3)	34.5(1.1)	1.46(2)	11.7(1)
$Q(2)$	6.1(5)	25.1(7)	7.7(2)	1.45(1)	3.8(2)
$Q(3)$	4.2(3)	13.5(3)	3.7(1)	0.51(1)	3.2(2)

[a]Ion signal amplitudes (arbitrary units). The numbers in parentheses, attached to each intensity, represent one standard deviation in the last figures quoted.

are tabulated by Bray and Hochstrasser.[20] The intensities of the O, Q, and S branches in a $^1\Sigma_g^+ - ^1\Sigma_g^+$ TP excitation by two linearly polarized (↑↑) photons are given by

$$I''[O(J)] = A(J)\frac{J(J-1)}{30(2J-1)}\left|s^{2,0}\right|^2 , \quad (4)$$

$$I''[Q(J)] = A(J)\left[\frac{1}{9}\left|s^{0,0}\right|^2 + \frac{J(J+1)}{45(2J-1)(2J+3)}\left|s^{2,0}\right|^2\right] , \quad (5)$$

$$I''[S(J)] = A(J)\frac{(J+1)(J+2)}{30(2J+1)(2J+3)}\left|s^{2,0}\right|^2 , \quad (6)$$

where the factor $A(J)$ includes the ground state rotational populations; and the second and zero rank tensors $s^{2,0}$ and $s^{0,0}$ are vibronic contributions to the intensities, and correspond to "zero trace symmetric tensor scattering" and "trace scattering," respectively, of Raman spectroscopy. In terms of the transition dipoles of Eq. (3), $s^{0,0}$ and $s^{2,0}$ can be expressed as

$$s^{0,0} = \mu_\parallel\mu_\parallel' + \mu_\perp\mu_\perp' , \quad (7)$$

$$s^{2,0} = 2\mu_\parallel\mu_\parallel' - \mu_\perp\mu_\perp' . \quad (8)$$

Therefore, for comparison of the experimental intensity distribution in a Q branch with theory, it is necessary to determine the relative values of $s^{0,0}$ and $s^{2,0}$. These are normally estimated by comparing the intensities of a Q line excited alternatively by linearly and circularly polarized radiation. For two-photon excitation by two circularly polarized (↻↺) photons is given by Eq. (9), and contains only the second rank tensor contribution:

$$I^{\circlearrowright\circlearrowleft}[Q(J)] = \frac{A(J)}{30}\frac{J(J+1)}{(2J+3)(2J-1)}\left|s^{2,0}\right|^2 . \quad (9)$$

In the case of $Q(0)$ line, Eqs. (5) and (9) predict for $I''/I^{\circlearrowright\circlearrowleft}$ a ratio of $\infty/1$, whereas the measured value is 9/1. It should be noted that because of the chromaticity of the Fresnel rhomb employed (cut for 219 nm) for transforming from linear to circular polarization, a ~10% residual contribution due to linear impurity in the circular polarization measurement, accounts for the observed deviation. Thus the above measurement is inaccurate for a determination of $s^{0,0}/s^{2,0}$.

A more reliable method in the present situation is to use the relative intensities of the Q and S members of a given band from Eqs. (5) and (6),

$$I''[Q(0)]/I''[S(2)] = 10.92_3\frac{\left|s^{0,0}\right|^2}{\left|s^{2,0}\right|^2} , \quad (10)$$

where $A(0)/A(2) = 1.2_4$ at 295 K. The measured rate is ~60 for the E–X (1, 0) band (at a sample pressure of 130 mTorr). [The $Q(0)$ and $S(2)$ lines are specifically used here since these are unperturbed, as shown previously]. We thus obtain

$$\left|s^{0,0}\right|^2 = 5.49\left|s^{2,0}\right|^2 , \quad (11)$$

from which it follows that the second term in Eq. (5) is insignificant and the Q branch rotational intensities should be determined primarily by the ground state population distribution. Equation (11) also enables one to determine the nature of the intermediate states. Substituting the expressions for $s^{0,0}$ and $s^{2,0}$ from Eqs. (7) and (8), we obtain

$$\frac{\mu_\perp\mu_\perp'}{\mu_\parallel\mu_\parallel'} = 1.1 \text{ or } 4.2 . \quad (12)$$

This ratio implies that the virtual intermediate state in the E–X (1, 0) TP process has significant contributions from $^1\Sigma_u^+$ and $^1\Pi_u$ states, with preference for the latter. An examination of the low-lying electronic states of H_2[1,27] shows that the most likely candidates are the $B\,^1\Sigma_u^+$ and $C\,^1\Pi_u$ states.

Next we consider the Q branch intensity distribution within each band. At 295 K, the calculated relative ground state populations in H_2 are 1 : 5.0 : 0.89 : 0.67 for $J'' = 0$–3. The experimental intensities, normalized to the $Q(0)$ value in each band, are depicted in Fig. 5. Within our measurement errors, the observed distributions reproduce the ground state populations only in the E–X (0, 0) band. The observed ratio for the E–X (2, 0) band (see Fig. 5) is 1 : 3.7(2) : 0.82(5) : 0.39(3), where the numbers in parentheses refer to the confidence limit of the last figure quoted. For the F–X (2, 0) and (4, 0) bands the ratios are, respectively, 1 : 5.8(6) : 5.7(4) : 2.0(2) and 1 : 4.3(4) : 1.4(2) : 1.2(2). All these ratios deviate from the expected trend. Although one cannot *a priori* entirely exclude the J dependence of the photoionization step, the observed deviations can be rationalized in terms of intramolecular perturbations. For example, the $v_E = 2$ and $v_F = 4$ levels interact extensively, on account of their proximity and the overlap of their wave functions. A similar but less extensive overlap occurs for the E–X(1, 0) and (F–X) (2, 0) bands. The proper comparison with expectation should therefore involve, for each J, the *average* of the intensities of these pairs of bands. In the case of the E–X (1, 0) and F–X (2, 0) transitions this ratio of the averages 1 : 4.6(2) : 1.1(1) : 0.64(3) agrees approximately with the expected values. For E–X (2, 0) and F–X (4, 0) however, the averages yield 1 : 3.8(3) : 0.95(5) : 0.57(5). The only serious discrepancy is in the $Q(1)$ value and can be accounted for by the proximity ($\Delta E \simeq 22.3$ cm^{-1}) of the $C\,^1\Pi_u$ $v = 2$, $J = 1$ and $E\,^1\Sigma_g^+$ $v = 2$, $J = 1$ levels.[6] This is thus expected to collisionally depopulate the interacting $v_E = 2$, $J = 1$ and $v_F = 4$, $J = 1$ levels.

For the purpose of comparing the observed $Q(0)$ intensities with theory, we invoke the usual sum rule to eliminate the sum over the vibrational levels of the intermediate states $|I\rangle$ [Eq. (3)]. This treatment is valid in the present case since there is no resonant one-photon state. Equation (3) thus reduces to

$$s_{k,l} = \langle v_T|v_G\rangle\left[\frac{\sum_i\langle t|\mu_k|i\rangle\langle i|\mu_l|g\rangle}{(E_I - E_G) - E_\omega + i\Gamma/2}\right] , \quad (13)$$

where $|t\rangle$, $|i\rangle$, and $|g\rangle$ represent the product of rotational and electronic parts of $|T\rangle$, $|I\rangle$, and $|G\rangle$, respectively; and $\langle v_T|v_G\rangle$ is a Franck–Condon factor. The TP vibronic intensity distribution is thus governed solely by the vibrational overlap integral $\langle v_T|v_G\rangle$. The relative vibronic intensities in our experiments are determined by the Franck–Condon factors for the TP excitation and the ionization step. The former can be calculated from the *ab initio* vibrational wave functions of Kołos and Wolniewicz,[9,23] and are given in square brack-

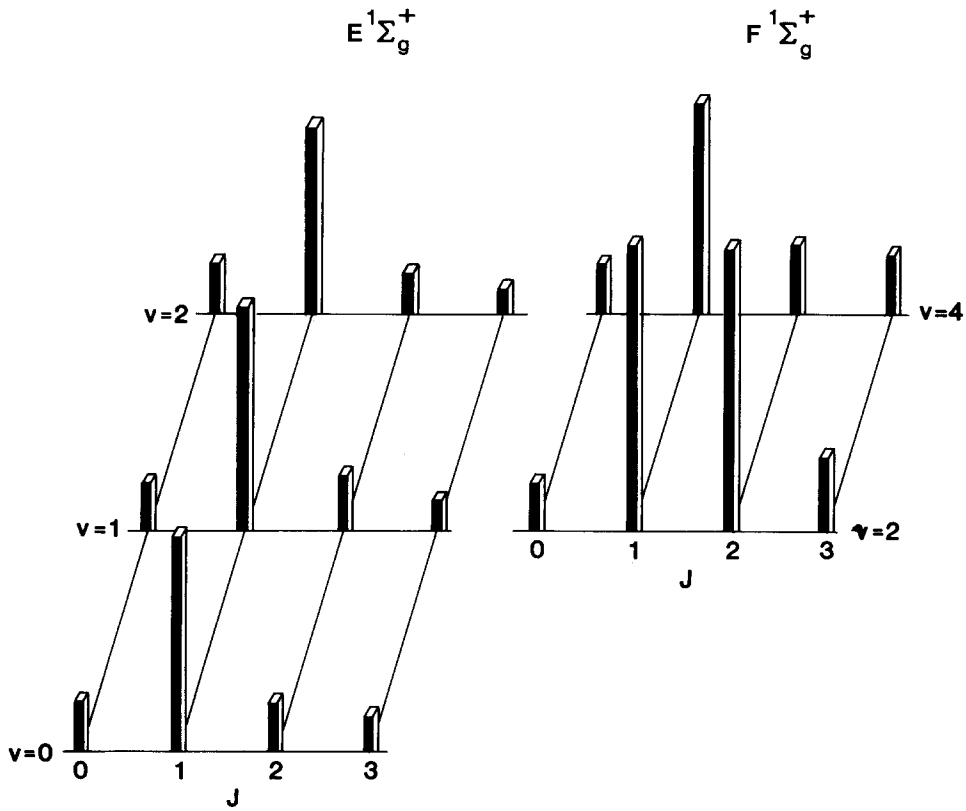

FIG. 5. Rotational line-intensity distributions for each band studied in this work. The Q-branch intensities have been normalized to the $Q(0)$ values in each band. Note that substantial departures from a simple Boltzmann distribution occur for all cases but the $E \rightarrow X$ (0, 0) band.

ets below each measured $Q(0)$ intensity in Table III. The observed relative $E-X$ (1, 0), (2, 0),and $F-X$ (2, 0), (4, 0) vibronic intensities are, respectively, about 3, 2, 7, and 2 times stronger than the calculated values. We suggest that this discrepancy may be associated with the ionization step. Since the wave function of $v_E = 0$ is localized in the $E\,^1\Sigma_g^+$ well and those of $v_E = 1$ and 2 tunnel into the $F\,^1\Sigma_g^+$ region, the results indicate that the photoionization from the outer well of the E, $F\,^1\Sigma_g^+$ state may be more efficient.

Finally, we address the question why transitions from $v_F < 4$ of the outer F well to the vibrational levels of the $B\,^1\Sigma_u^+$ state were not previously observed in the studies of Dieke[4-8] or of Watson and Anderson.[12] In both experiments the production of the E, F state involves: (a) the formation of high electronic states of H_2 either directly by electron impact or by recombination of H_2^+ and e^-; and (b) radiative cascade to the E, F state. The preferential population of the inner E well can be ascribed to the larger vibrational overlaps of the various electronic states of H_2 with the inner well levels. The observation of $v_F = 4$ is not inconsistent with this picture since the vibrational wave function of this level has a large amplitude in the Franck–Condon-favored region.[9] For $v_F < 4$, the vibrational overlaps are much smaller. Moreover, the $F-B$ emission from $v_F < 4$ should peak around 1 μm where it is probably masked by other stronger electronic transitions. The ability of the present method to observe the $v_F = 2$ and 3 levels is a consequence of its inherent sensitivity. This technique could be extended to the study of higher excited states of H_2, such as the G, $K\,^1\Sigma_g^+$ state, which is also thought[10,11] to possess a double minimum.

ACKNOWLEDGMENT

We thank K. Dressler for valuable comments on this work.

[1] K. P. Huber and G. Herzberg, *Constants of Diatomic Molecules* (Van Nostrand Reinhold, New York, 1979).
[2] E. R. Davidson, J. Chem. Phys. **33**, 1577 (1960); **35**, 1189 (1961).
[3] O. W. Richardson, *Molecular Hydrogen and its Spectrum* (Yale University, New Haven, Connecticut, 1934).
[4] G. H. Dieke, Phys. Rev. 50, 797 (1936).
[5] G. H. Dieke, Phys. Rev. 76, 50 (1949).
[6] G. H. Dieke, J. Mol. Spectrosc. 2, 494 (1958).
[7] G. H. Dieke and S. P. Cunningham, J. Mol. Spectrosc. **18**, 288 (1965).
[8] H. M. Crosswhite, *The Hydrogen Molecular Wavelength Tables of Gerhard Heinrich Dieke* (Wiley–Interscience, New York, 1972).
[9] W. Kołos and L. Wolniewicz, J. Chem. Phys. 50, 3228 (1969).
[10] L. Wolniewicz and K. Dressler, J. Mol. Spectrosc. 67, 416 (1977).
[11] K. Dressler, R. Gallusser, P. Quadrelli, and L. Wolniewicz, J. Mol. Spectrosc. 75, 205 (1979).
[12] J. Watson, Jr., and R. J. Anderson, J. Chem. Phys. 66, 4025 (1977).

[13]I. Dabrowski and G. Herzberg, Can. J. Phys. **54**, 525 (1976).
[14]D. J. Kligler and C. K. Rhodes, Phys. Rev. Lett. **10**, 309 (1978); D. J. Kligler, J. Bokor, and C. K. Rhodes, Phys. Rev. A **21**, 607 (1980).
[15]E. E. Marinero, C. T. Rettner, and R. N. Zare, Phys. Rev. Lett. **48**, 1323 (1982).
[16]I. Deĕzsi, Acta Phys. Acad. Sci. Hung. **9**, 125 (1958); L. Gero and R. Schmid, Proc. Phys. Soc. **60**, 533 (1948).
[17]B. L. Stoicheff, Can. J. Phys. **35**, 730 (1957). There may be a pressure shift correction needed because Stoicheff's measurement refers to a low pressure H_2 sample. However, the value of the (1,0) band origin of the E–X system determined here differs by only 0.03 cm^{-1} from that obtained from Ref. 6 using the B–X measurements of Ref. 20 (see Ref. 21). This implies that the pressure shift correction is smaller than our measurement error.
[18]R. G. Bray and R. M. Hochstrasser, Mol. Phys. **31**, 412 (1976).
[19]W. M. McClain and R. A. Harris, in *Excited States*, edited by E. C. Lim (Academic, New York, 1977), Vol. 3, pp. 1–56.
[20]G. Herzberg and L. L. Howe, Can. J. Phys. **37**, 636 (1959); P. G. Wilkinson, *ibid.* **46**, 1225 (1968).
[21]The E, F state term values listed by Dieke (Ref. 6) were obtained from E, F–B line positions and B–X measurements of Richardson (Ref. 3), but the latter values differ from the improved measurements of Ref. 20 by ~8 cm^{-1}, as discussed previously in Ref. 10. This discrepancy, unfortunately, was not noted in recent TP studies of H_2 (Refs. 14 and 15) who used Dieke's term values.
[22]K. Dressler (private communication).
[23]B. Ritchie, E. J. McGuire, J. M. Peck, and C. W. Hand, J. Chem. Phys. **77**, 877 (1982).